Progress In Electromagnetics Research B, Vol. 14, 1–21, 2009

SOIL IONIZATION DUE TO HIGH PULSE TRANSIENT CURRENTS LEAKED BY EARTH ELECTRODES

G. Ala, M. L. D. Silvestre, and F. Viola

Dipartimento di Ingegneria Elettrica
Elettronica e delle Telecomunicazioni, viale delle Scienze
Università degli Studi di Palermo
Palermo 90128, Italia

E. Francomano

Dipartimento di Ingegneria Informatica, viale delle Scienze
Università degli Studi di Palermo
Palermo 90128, Italia

Abstract—This paper proposes a numerical model of the soil ionization phenomena that can occur when earth electrodes are injected by high pulse transient currents, as the one associated with a direct lightning stroke. Based on finite difference time domain numerical scheme, this model ascribes the electrical breakdown in the soil to the process of discharge in the air. In fact, as soon as the local electric field overcomes the electrical strength, the air in the voids trapped among soil particles is ionized, and the current is conducted by ionized plasma paths locally grown. The dimension of these ionized air channels is strictly dependent upon the local temperature. Thus, a local heat balance is enforced in order to obtain the time variable conductivity profile of the medium. This model can be implemented both for concentrated and extended electrodes, since no hypothesis has to be enforced about the geometric shape of the ionized region. Validation of the proposed model is obtained by comparing simulation results with experimental data found in technical literature.

Corresponding author: G. Ala (guido.ala@unipa.it).

1. INTRODUCTION

The electromagnetic (EM) characterization of earth electrodes under high pulse transient currents is an important highpoint in the design of a grounding system, especially when it is a part of a lightning protection system (LPS). It is well known that a direct or indirect lightning stroke could produce dangerous conditions for human body, as well as unwanted electromagnetic interferences among electrical and electronic systems. The LPS has to be designed to minimize these hazardous effects. Especially, the earth termination system, should be designed in order to avoid danger to people by minimizing dangerous transient step and touch voltages on the ground surface, and to limit the voltage between any two points of the earth electrode.

In order to simulate the transient behavior of simple earth electrodes, wire antenna model can be used [1, 2]. Advanced numerical models enable to investigate transient performances of extended earth electrodes [3–5] and the whole LPS [6].

Moreover, high pulse transient current can cause the electric field on the surface of the electrode to overcome the electrical strength in the soil. Thus, ionization phenomena can occur and the EM transient performance of the global system is modified with respect to the case of absence of soil breakdown. In fact, in the soil zones affected by ionization the value of the conductivity considerably increases with respect to its value obtained with low magnitude and low frequency input, so modifying the current path. Original low frequency values of soil parameters are restored only at the end of the subsequent de-ionization process. Thus, it is extremely useful to take into consideration the real soil behaviour during the breakdown phenomenon, in order to correctly design the earth electrodes.

With the aim to take into account the nonlinear effects due to soil ionization, different models are available in technical literature [7–19]. Basically, they can be classified as the variable geometry approach and the variable soil conductivity approach.

In the first case, by considering an embedded electrode in an ionized soil, the study is carried out with an electrode of modified transversal dimensions into a non-ionized soil [7–13]. A time variable radius of the electrode is set by imposing that the electric field at the electrodes surface may not exceed the electrical strength. This is based on the hypothesis that, when the ionization process starts, the soil conductivity in the ionized zone, supposed to be uniform around the electrodes, instantaneously assumes the electrode conductivity value. As a consequence, the time variable radius of the electrode is expanded up to a distance where the electric field is decreased below the electrical

strength. However, in authors' opinion, this model is quite far from the real ionization mechanism, since the ionized zones of the soil around the electrodes are considered well-shaped and substituted by an electrode of larger dimension and having a prefixed conductivity value.

In authors' opinion, a more realistic approach is the one based on variable soil conductivity [14–19]. Originally in [14], the ionized soil conductivity is expressed as a nonlinear time function when the local electric field exceeds the electrical strength. Some hypotheses are adopted in order to obtain the effective time profile of the soil resistivity during the subsequent de-ionization process [14]. In such a way, the soil resistivity in the ionized zone is assumed to decrease to some percentage of its pre-ionization value. Similarly, the other papers based on the variable soil conductivity approach [15–19] allow to study the ionization phenomenon by considering global parameters as potential to remote ground and LPS global resistance. However, also for the variable soil conductivity approaches found in literature, some hypotheses about the shape of the ionized region around the electrodes have to be enforced [14–19].

Thus, new efforts have to be constantly provided in order to better reproduce the physical ionization mechanism and to obtain more accurate models.

In order to overcome the need of formulating some hypotheses about the shape of the soil ionized zones around the electrodes, numerical solution of Maxwell's curl equations can be used in time domain. In [20], based on the space-time variable soil conductivity approach reported in [14], a finite difference time domain (FDTD) numerical scheme is proposed, so obtaining a local description of the soil ionization and de-ionization processes. In this approach, it is not necessary to predetermine the shape of the ionized regions, since these shapes are naturally built in the region under study during the time steps and driven by the actual local value of the total electric field.

As a further fundamental step towards a more accurate analysis of the real ionization mechanism, in this paper a model developed from a thorough analysis of the available studies in technical literature, about the peculiar physical dynamics of soil ionization phenomena, is proposed. It is worked out by processing together a useful physical model of soil ionization available in literature [21] and the FDTD scheme already developed in [20]. This model ascribes the soil ionization phenomenon to the electrical discharge in the air trapped in the voids among solid soil particles, and can be enumerated among the models which support a variable soil conductivity. When the electric field overcomes the electrical strength, soil ionization occurs, and the conductive plasma paths locally grow. The dimensions of these ionized

air channels are strictly dependent upon the local temperature. So, a local heat balance is enforced in order to obtain the actual value of the medium conductivity. This heat balance is evaluated instantaneously in each lattice cell of the region of interest, if the actual electric field value overcomes the electrical strength.

Validation of the proposed model is obtained by comparing simulation results with experimental data found in technical literature [13, 14, 17, 21]. In authors' opinion, the proposed model represents a general tool to analyze, with a more physical emphasis with respect to what is presented in literature, the EM nonlinear transient behaviour of earth electrodes: the analysis can be carried out even if the electrodes have complex geometry or are embedded in a stratified soil, and without any apriori hypothesis about the shape of the ionized zones.

2. THE PHISYCAL SOIL IONIZATION MODEL

It is well known that soil ionization phenomena can occur when earth electrodes are injected by high pulse transient currents. The ionization process begins as soon as the current leaked into the soil, which is high enough to let the electrical field on the electrodes surface overcome the electrical strength, so modifying the behavior of the electrode with respect to the absence of soil ionization.

Since the soil ionization is an extremely complicated nonlinear process, some approximations are usually adopted. The soil is often considered to be homogeneous and isotropic. Consequently, ionization is assumed to be uniform in the soil around the electrodes, and some hypotheses about the ionized zone shape are enforced, as already underlined.

Ionization phenomenon is a local process that begins in those areas where the density of the current leaked into the soil has reached higher values and where conductive plasma paths can locally grow. Because of the structure of the soil, it is very unlikely that regular and uniform ionized zones can result. In fact most soils consist of a mixture of small and not conductive grains, water and air [22]. The water and air fill up the vacuity among the solid pieces, forming a large and close net. The interconnection of water layer generates conductive channels, which are the cause of the high soil conductivity value. Indeed, the soil electric conductivity is a very variable parameter, depending on the size and the distribution of the not conductive particles, on the amount of water and on the amount of salt dissolved in the water. The grains have very different sizes and often have irregular shapes. Therefore, the air gaps within the soil have highly irregular shape, especially if the surrounding pieces have sharp edges. This makes the

maximum electric field inside the air voids within the soil significantly higher than the maximum electric field within the voids of an air gap having the same average size [22]. So, the field enhancement in voids enclosed within the soil can be reasonably considered as the cause for the beginning of the ionization process in the soil.

According to these considerations, the process begins when the electric field impressed on air gaps among soil grains, which becomes large enough to ionize the air in the void. Then, the soil breakdown mechanisms can be ascribed to the electrical discharges within air gaps trapped in the soil; these discharges spread from the electrode surface and may be more and more branched.

This supposition is confirmed by experimental results [11, 19] on soil discharges devoted to investigate the effects on the electric characteristics of the soil due to the impressed voltage pulse polarity, grain size and degree of humidity. These results are in agreement with the studies on electrical discharges in air.

According to the previous considerations, in [21] the discharge into the soil is ascribed to a discharge in air by linking ionization phenomenon to a strong heating of the air trapped inside the soil. The breakdown process can be separated in two phases. The first, the pre-ionization phase, consists in the propagation of streamers across the air gaps, the subsequent rearrangement of the charge in the streamers and the heating and the expansion of these channels. During this stage, the channel temperature can reach a few thousand Celsius degrees. In the second phase, the current and the temperature in the channel increase, and the considerable thermal ionization causes spark starting.

As already underlined, this approach can be classified as one of those models supporting the soil conductivity around earth electrodes as a variable. In fact, the ionized channels conductivity in the soil surrounding the earth electrodes is assumed to be a function of the current flowing through them; it is calculated by taking into account the balancing between the heat generation and the heat dissipation of the channels. Moreover, the air conductivity is considered as a function of the local temperature.

The model proposed in [21] seems to be very close to the physical mechanism of soil ionization phenomenon. However in [21], some hypotheses about the shape of the ionized region surrounding the electrodes are introduced, and only the global surge impedance is taken into account, with reference to a concentrated earth.

In order to overcome the difficulty of a correct guess of the ionized zone, this physical approach has been revised and integrated into an FDTD numerical scheme, which enables to evaluate the actual local electric field in the elementary cell of the lattice used to schematize

also the part of medium interested by the ionization process. The aim is to obtain the actual value of the medium conductivity. This is carried out by enforcing, instantaneously, a local heat balance, when the electric field overcomes the electrical strength. According to [21], when the electric field in the soil overcomes the electrical strength, an instantaneous pre-ionization phase is supposed to create highly conductive discharge channels at a fixed temperature, i.e., 3600 K as reported in [21]. Then, the energy dissipated inside the channels increases the temperature of the air.

Because of the balancing between the heat generation and the heat dissipation of the channels, the air trapped in the soil can reach very high temperature.

Several studies are available in scientific literature about thermodynamic properties and transport coefficients of air in a wide range of temperature and pressure values, referred to calculated models or experimental investigations. From these data, it is possible to obtain the conductivity of air inside these channels as a function of the temperature [23–25].

3. SOIL IONIZATION MODEL IN A FDTD SCHEME

The previous approach [21] has been integrated into a FDTD numerical scheme. Therefore, grounding system and surrounding soil are segmented into a lot of box-shaped elementary cells. Then, the EM field within the investigated zone is mapped in space, by discretization of the curl Maxwell's equations, and by mapping them by implementation of the central-difference leapfrog Yee's scheme [26–28]. Likewise, following the Yee's algorithm, the electric and magnetic fields are updated in time at alternate half time steps: First the electric field, then the magnetic one are computed at each time step Δt. The soil conductivity is considered time varying by assuming the following hypotheses. Inside each elementary cell of the FDTD grid, it is possible to separate the material substances forming the soil from air voids: For the first ones the electrical conductivity is given by interlinked water path covering soil grains and it is assumed constant during the ionization process; for the air voids, it is supposed that the electrical conductivity varies with the temperature. The division of soil in two elements (ΔA_S and ΔA_A) has been sketched in Fig. 1.

Thus the current flowing into the soil finds two different parallel ways and the average conductivity can be expressed as a function of the temperature, as follows:

$$\sigma(T) = \left\{\sigma_S \Delta V_S + \sigma_A\left(T\right) \Delta V_A \left(T/T_a\right)\right\} / (\Delta V_S + \Delta V_A) \qquad (1)$$

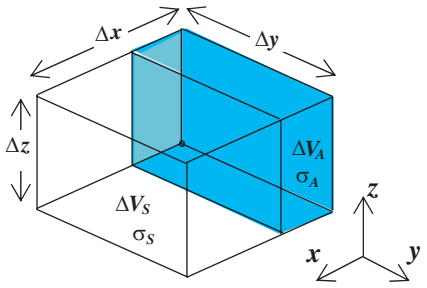

Figure 1. Elemental cell. Soil grains and air voids have different volumes and different conductivities. (A index as air; S index as soil).

where: σ_s is the steady state soil conductivity; T is the actual value of air temperature; $\sigma_A(T)$ is the air conductivity as a function of temperature; T_a is the soil temperature before the ionization takes place and the temperature of the surrounding cells ($T_a = 25°\text{C}$).

Moreover, since no information is required from the knowledge of magnetic field, the evaluation of the novel conductivity value has to be embedded between the computation of the electric field cell's and that of the magnetic field cell's. Thus, at each time step, at first the electric field $\mathbf{E}^n_{x,\,y,\,z}$ is evaluated, then the value of conductivity σ^n, and finally the magnetic field $\mathbf{H}^{n+1/2}_{x,\,y,\,z}$ are updated: n as the actual time step $n\Delta t$; x, y, z, as the actual spatial position.

If the local total electric field, $\mathbf{E}^n_T$, overcomes the electrical strength $\mathbf{E}_c$, the ionization phenomena inside the elementary cell occurs and the instantaneous pre-ionization phase produces highly conductive discharge channels at a fixed temperature (i.e., 3600 K [21]). Then the local dynamic heat balance is enforced in order to describe the physical phenomenon, and the corresponding actual air conductivity is computed.

Regarding the power-loss mechanism and energy storage in the dynamic arc-plasma phenomena, it is useful to refer to Cassie's model [29]. In order to plasma condition the requiring energy, ΔW^n_p, to support the arc in the elementary volume ($\Delta V = \Delta x \Delta y \Delta z$) at the generic time step n, is:

$$\Delta W^n_p = \sigma^{n-1}_A \mathbf{E}^2_c \Delta V \Delta t \tag{2}$$

where $\mathbf{E}_c$ is the electrical strength; σ^{n-1}_A is the air conductivity at the previous time step $(n-1)$. Therefore, the generated energy in the elementary plasma channel is:

$$\Delta W^n_E = \sigma^{n-1}_A \left[(\mathbf{E}^n_T)^2 - (\mathbf{E}_c)^2 \right] \Delta V \Delta t \tag{3}$$

where $\mathbf{E}_T^n$ is the total electrical field at time step n.

This available energy (3) is not totally employed to increase the cell's temperature, since a heat exchange between plasma stream and surrounding material happens. Then, the local energy instantaneously dissipated in the medium, reduced by the heat transmitted out of the cell, is considered to drive the temperature gradient of the plasma channel.

Such heat balance is affected by many factors: Among them, temperature, dimension of plasma stream and also the actual pressure value.

A temperature-depending volume of the plasma channel, as a fraction of the global volume of the cell, has been used by considering the following [21]:

$$V_a(T) = 0.005 \cdot (T/T_a) \tag{4}$$

Minor approximations have been introduced in the evaluation of the transmitted heat. The dissipating heat surface of the plasma channel has been obtained by taking into account the six faces of the Yee's cell multiplied by (4), and a heat transfer coefficient, $S = 25\,[\mathrm{Wm^{-2}K^{-1}}]$, has been set. The value of S has been chosen equal to the medium value of the heat transmission coefficient of the air, found in thermodynamic literature, and it is assumed to be constant, as a first approximation. In such a way, the transmitted heat ΔW_t is expressed by the following:

$$\Delta W_t^n = S \cdot V_a(T^{n-1}) \cdot 2(\Delta x\Delta y + \Delta x\Delta z + \Delta x\Delta z)\left(T^{n-1} - T_a\right)\Delta t \tag{5}$$

where T^{n-1} is the temperature at time step $(n-1)$. Equation (5) is obtained by supposing that the space surrounding the cell always has the same temperature T_a, as a first approximation. The temperature gradient is computed by subtracting the transmitted heat from the total available energy and by considering the specific heat capacity $C_p = 1.005\,[\mathrm{kJ/kgK}]$, which is assumed to be constant. The temperature variation can be then expressed as:

$$\Delta T = \frac{\Delta W_E^n - \Delta W_t^n}{V_a(T^{n-1}) \cdot \Delta V \cdot \delta\left(T^{n-1}\right) \cdot C_p} \tag{6}$$

where the air density $\delta(T)$ has been introduced:

$$\delta(T) = \frac{p}{0.287 \cdot T} \tag{7}$$

with $p = 101.325$ [kPa]. Thus, the actual temperature T^n of the cell is:

$$T^n = T^{n-1} + \Delta T \tag{8}$$

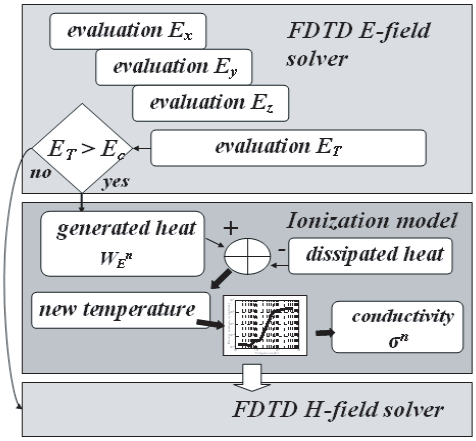

Figure 2. The evaluation of the new cell's conductivity is set between the electric field and magnetic field computations.

Finally, by considering (8) and the experimental data reporting the conductivity values of air as a function of temperature [23–25], it is possible to obtain σ_A^n. Fig. 2 shows the used ionization time stepping computational scheme.

In order to avoid numerical instability in the FDTD algorithm, the sampling time ΔT has been chosen in accordance with Courant, Friedich, Levy (CFL) condition [18]:

$$\Delta T = 1/\left(u_{\max} \cdot \sqrt{1/\Delta x^2 + 1/\Delta y^2 + 1/\Delta z^2}\right) \tag{9}$$

where $u_{\max}$ is the maximum wave phase velocity within the model.

Moreover, since the simulation of transient performance of earth electrodes represents an open boundary EM problem, in order to avoid spurious reflections due to cutting off of the grid, the Berenger Perfectly Matched Layer (PML) has been implemented in the computer code as appropriate boundary conditions [28].

4. VALIDATION OF THE PROPOSED MODEL

In order to validate the proposed model, a comparison with experimental results found in technical literature has been carried out. In particular the dynamic behavior of a 0.61 m rod and radius equal to 6.35 mm, embedded in homogeneous soil ($\rho_0 = 50\,\Omega$m; $\varepsilon_r = 8$;

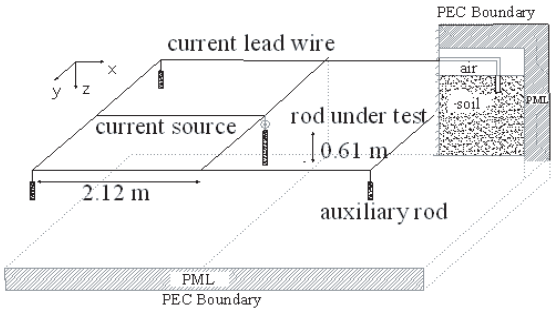

Figure 3. A single rod embedded in homogeneous soil: Four auxiliary rods are used in order to build the current return path.

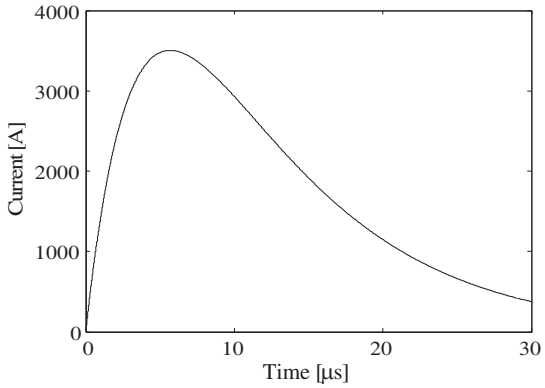

Figure 4. Double exponential current waveform adopted in [14] (p. 127, Fig. 3(c)) and used for the simulation.

$\mu = \mu_0$), has been investigated (Fig. 3). This scenario is the same as that reported in [14].

Since the rod is simulated with a thin-wire perfect conductor, according to the FDTD simulation-techniques, the "intrinsic radius" concept [30] has been used and the radius of the rod has been set to $r_0 \approx 0.012\,\mathrm{m}$.

The rod is directly fed by an ideal surge current generator. A double exponential $4\,\mu\mathrm{s}/18\,\mu\mathrm{s}$, $3500\,\mathrm{A}$ impulse waveform has been employed (Fig. 4), and the electrical strength is set to $\mathbf{E}_c = 1.1\,\mathrm{kV/cm}$.

The comparison between the behavior achieved by Darveniza and the one obtained with the proposed model, is shown in Figs. 5 and 6.

A second level of validation has been acquired by comparing the

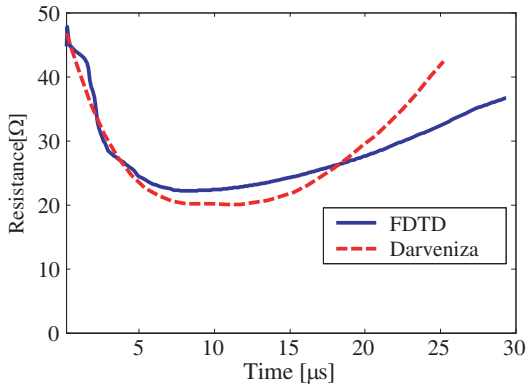

Figure 5. Transient earth resistance profile of the rod sketched in Fig. 4.

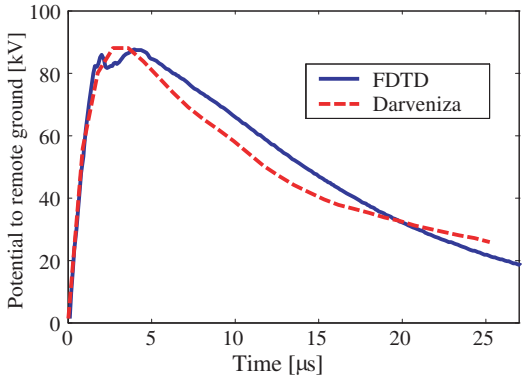

Figure 6. Potential to remote ground time profiles of the input section of the rod sketched in Fig. 3.

results of the presented model with those found in [14] and [21]. In this case, the dynamic behavior of a 3.05 m single vertical rod with a 0.0127 m radius has been investigated. In Fig. 7, the adopted current time profile is shown. The rod is embedded in a homogeneous soil, $\rho_0 = 87\,\Omega$m, $\varepsilon_r = 8$, $\mu = \mu_0$, $\mathbf{E}_c = 1.27\,$kV/cm. Fig. 8 shows the comparison among experimental data (obtained also by the model of Cooray [21]), Darveniza's model and the FDTD computation. All the time profiles are close to each other.

In order to test the flexibility of the proposed model a more complex simulation has been set. Recently in [17], the behavior of stratified soils has been studied. Stratified soils approximate the particular moisture of the soil due to the climatic conditions in different

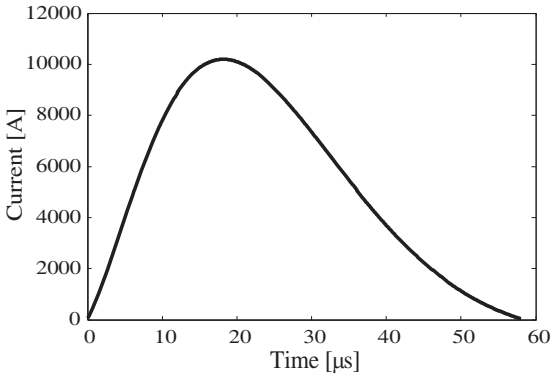

Figure 7. Double exponential waveform adopted in [8] (p. 129, Fig. 6) and in [17] (p. 197, Fig. 2), and also used for the simulation.

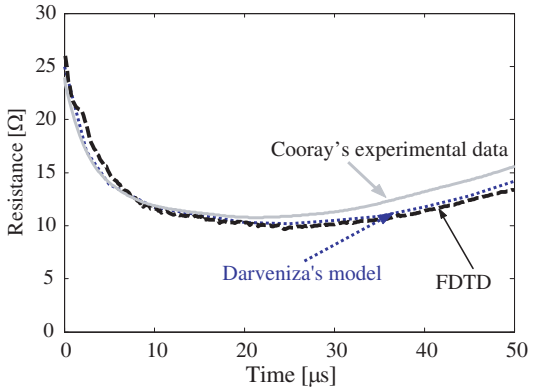

Figure 8. Transient earth resistance time profile of the rod.

countries: In the northern regions in winter the upper layer of the soil becomes frozen and its resistivity results much higher than the one in the bottom, while in the southern regions the upper layer of the soil is wetter than the bottom layer and it has a lower resistivity. In the summer these conditions can be reversed due to the effects of the heat. The simulation of a two stratified soil geometry has been built by following what reported in [17]. The first layer has a thickness of 0.8 m with a high resistivity, $\rho_0 = 2000\,\Omega$m and its critical electric field $\mathbf{E}_c$ is set 1000 kV/m, while the bottom layer has a low resistivity, $\rho_0 = 42\,\Omega$m, and $\mathbf{E}_c = 350$ kV/m. Each soil has the same relative permittivity, $\varepsilon_r = 10$, and a one meter vertical rod, with 50 mm

diameter, has been injected by the following waveform current:

$$i(t) = 10000\left(e^{-14300t} - e^{5400000t}\right) \tag{10}$$

A spatial uniform step $\Delta x = 0.20\,\mathrm{m}$ has been set in order to better approach the geometry of the problem. By following what reported in [17], a comparison among different scenarios has been carried out. Two more limit cases have been considered by neglecting the ionization phenomenon: one with a homogeneous soil with the higher resistivity value and the other with m.x200=the lower one. The obtained results have been depicted in Fig. 9 in terms of potential to remote ground of the injected point of the rod. The upper curve is representative of the potential to remote ground of the system in which the soil is homogeneous and the resistivity is set to a higher value, while

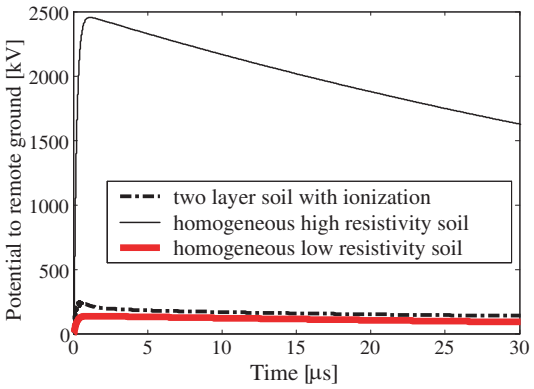

Figure 9. Transient potential to remote ground of the rod with different soil scenarios.

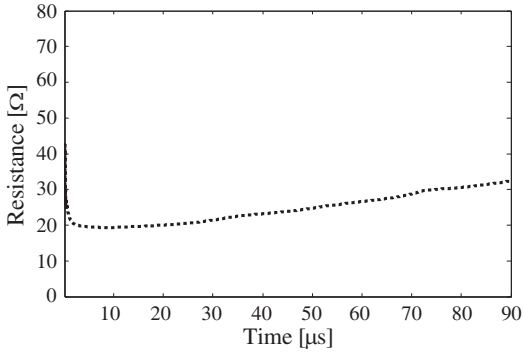

Figure 10. Transient resistance time profile for two-layer soil with ionization.

the bottom curve represents the behavior of a homogeneous low resistivity soil. The two-layer soil behavior with soil ionization model is represented by the intermediate curve. As obtained in [17], the time profile of the low resistivity soil is close to that obtained with the ionized two-layer soil.

In Fig. 10, the time profile of transient rod resistance with the two-layer soil scenario in presence of ionization has been plotted. The reached minimum value is close to the stationary low frequency value of the lower resistivity soil, i.e., about $14\,\Omega$.

It is useful to summarize the results obtained with all the cases studied into a table, by considering the variation of the peaks of potential to remote ground in presence of soil ionization referred to those obtained without considering soil ionization (Table 1).

Table 1. Variation of potential to remote ground peak value in presence of soil ionization with respect to absence of ionization.

Case study	Peak current [kA]	Low frequency resistance R_{AC} [Ω]	$\Delta V\%$
Rod as in [14] (p. 127, Fig. 3(c))	3.5	51.5	45.10
Rod as in [21] (p. 197, Fig. 2)	11	24.9	55.60
Rod as in [17] (p. 208, Fig. 4)	10	31.1	37.01

5. PARAMETRIC ANALYSIS

The transient behavior of the earthed electrodes is affected by different parameters, such as the moisture of the soil, dimension of soil grains, water and salt content, and geometrical characteristics of the electrodes. These parameters influence the soil resistivity value, the electrical strength value, and the subsequent ionization phenomenon. In order to obtain an overview of the influence of these parameters on the behavior of the earthed electrode, further different scenarios have been simulated, also to show the potentiality of the proposed model.

Let us consider the system reported in [18]. A 1.5 m single vertical rod with a 7 mm radius, has been investigated. The rod is embedded in a homogeneous soil, $\rho_0 = 160\,\Omega$m, and $\mathbf{E}_c = 3.5\,$kV/cm. The low frequency resistance, R_{AC}, is about $92\,\Omega$. The rod is injected by the current sketched in Fig. 11.

In this case, the computed reduction of potential to remote ground peak value with soil ionization is about 55% with respect to the case without considering the ionization phenomenon. By considering the

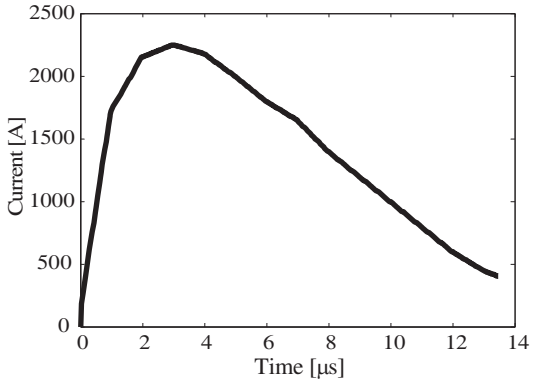

Figure 11. Current waveform adopted in [18] (p. 195, Fig. 3(a)) and used for the simulation.

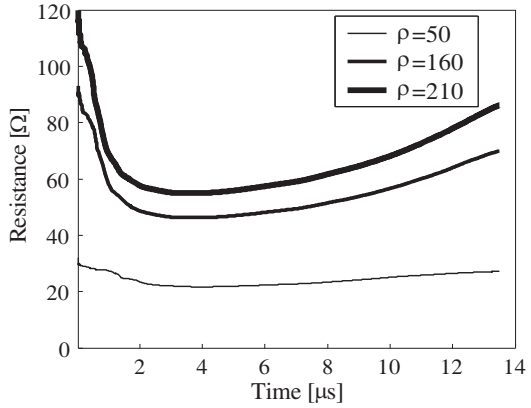

Figure 12. Transient potential to remote ground of the rod for different homogenous soil scenarios.

influence of the low frequency resistivity value, which varies with the amount of water in the soil, three different moisture cases have been taken into account:

- soil A, $\rho_0 = 50\,\Omega$m, $\mathbf{E}_c = 3.5\,$kV/cm, $R_S = 28\,\Omega$;
- soil B, $\rho_0 = 160\,\Omega$m, $\mathbf{E}_c = 3.5\,$kV/cm, $R_S = 92\,\Omega$;
- soil C, $\rho_0 = 210\,\Omega$m, $\mathbf{E}_c = 3.5\,$kV/cm, $R_S = 120\,\Omega$.

It has to be underlined that similar variations can be achieved due to variable climatic conditions. A clayey soil can reach a lower resistivity than soil A in wet conditions, and in dry condition its resistivity is similar to that of soil C. By considering the ionization

phenomenon, in Fig. 12, the different time profiles of the computed transient input resistance have been sketched. In Table 2, the comparison of the variation of the peak values of potential to remote ground in presence of soil ionization referred to the absence of it is reported. Table 2 shows that the greater contribution in the reduction of the relative voltage peak is for the higher resistivity soil (soil C).

Table 2. Variation of potential to remote ground in presence of soil ionization.

Case study	Low frequency resistivity [Ωm]	Voltage peak [kV]	$\Delta V\%$
Soil A	50	50	18.63
Soil B	160	110	42.86
Soil C	210	124	50.07

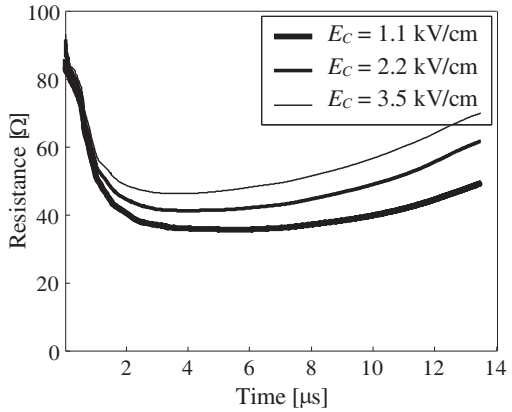

Figure 13. Transient resistance of the rod in different soil conditions.

By considering the electrical strength value, which varies with the size and shape of soil grains [22], three different soils have been taken into account:

- soil D, $\rho_0 = 160\,\Omega$m, $\mathbf{E}_c = 1.1\,$kV/cm;
- soil E, $\rho_0 = 160\,\Omega$m, $\mathbf{E}_c = 2.1\,$kV/cm;
- soil B, $\rho_0 = 160\,\Omega$m, $\mathbf{E}_c = 3.5\,$kV/cm.

Figure 13 shows the input resistance time profiles for the three different scenarios, obtained by imposing separately the three previous

addressed values of the electrical strength; the earth electrode and the low frequency soil conductivity value are considered unchanged for these computations. The obtained results show that the soil ionization is more stressed when the electrical strength is set to the lower value. These results are in accordance with the physical behaviour of the soil since a lower value of the electrical strength, with the other parameters being unchanged, enables the soil ionization mechanism to take place in an easier way, because Ec is governed by the air in the voids [22]. In fact, with a lower electrical strength, a larger volume of soil around the electrode is affected by an electric field value greater than Ec: thus, a more stressed soil breakdown into air channels takes place so reducing the transient resistance values. In Table 3, the comparison of the variation of the peak values of potential to remote ground in the presence of soil ionization referred to the absence of it, is reported. Again, the variation is higher when the electrical strength is set to the lower value.

In order to investigate the influence of the geometric parameters on the electrode performance, in the following simulation the soil B (160 Ωm, $\mathbf{E}_c = 3.5\,\mathrm{kV/cm}$) and three rods with different length have been taken into account:

- rod A, 7 mm radius, 0.75 m length;
- rod B, 7 mm radius, 1.50 m length;
- rod C, 7 mm radius, 3.00 m length.

Figure 14 shows the transient input resistance time profiles. A more accentuated ionization happens with the shortest rod, because the current density increases as the rod length decreases.

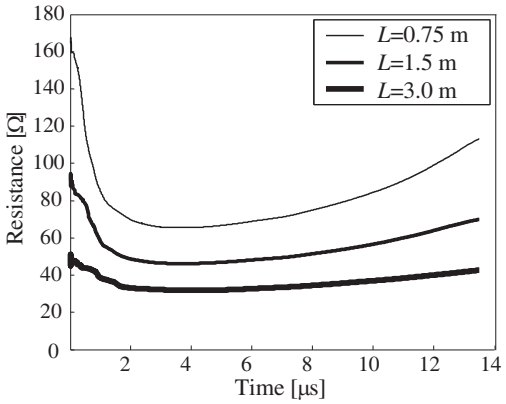

Figure 14. Transient input resistance of the rods.

The variation is higher for the rod of lower length.

Table 3. Variation of potential to remote ground in presence of soil ionization.

Case study	Electrical strength [kV/cm]	Voltage peak [kV]	$\Delta V\%$
Soil D	1.1	90	52.52
Soil E	2.1	96	49.62
Soil B	3.5	110	42.86

Table 4. Variation of potential to remote ground in presence of soil ionization.

Case of study	Rod length [m]	Voltage peak [kV]	$\Delta V\%$
Rod A	0.75	150	53.34
Rod B	1.50	110	42.86
Rod C	3.00	72	32.45

6. CONCLUSIONS

In this paper, a numerical approach of the soil ionization phenomena that can occur when earth electrodes are injected by high pulse transient currents has been proposed. It is based on a mixed thermal/electromagnetic model solved by the FDTD scheme. The results reported in the previous sections enable to demonstrate the validity and the potentiality of the proposed computational tool. The choice of considering only single rod arrangements has been due to the possibility of successfully compare the results of the proposed model with those reported in technical literature. However, more complex systems can be straightforwardly simulated. In authors' opinion, the proposed model enables to simulate the electromagnetic transient performance of earth electrodes subject to high current pulse, in a more realistic way with respect to what reported in technical literature.

ACKNOWLEDGMENT

This work has been supported by the Italian "MInistero dell'Istruzione dell'Università e delle Ricerca" (MIUR).

REFERENCES

1. Poljak, D. and V. Doric, "Wire antenna model for transient analysis of simple grounding systems, Part II: The horizontal grounding electrode," *Progress In Electromagnetics Research*, PIER 64, 167–189, 2006.
2. Poljak, D. and V. Doric, "Wire antenna model for transient analysis of simple grounding systems, Part I: The vertical grounding electrode," *Progress In Electromagnetics Research*, PIER 64, 149–166, 2006.
3. Grcev, L. and F. Dawalibi, "An electromagnetic model for transients in grounding systems," *IEEE Trans. on Power Delivery*, Vol. 5, No. 4, 1773–1781, Oct. 1990.
4. Dawalibi, F., W. Xiong, and J. Ma, "Transient performance of substation structures and associated grounding systems," *IEEE Trans. on Industry Application*, Vol. 31, No. 3, 520–527, May/Jun. 1995.
5. Grcev, L., "Computer analysis of transient voltages in large grounding systems," *IEEE Trans. on Power Delivery*, Vol. 11, No. 2, 815–823, Apr. 1996.
6. Ala, G. and M. L. Di Silvestre, "A simulation model for electromagnetic transients in lightning protection systems," *IEEE Trans. on Electromagnetic Compatibility*, Vol. 44, No. 4, 539–554, Nov. 2002.
7. Geri, A., "Behaviour of grounding systems excited by high impulse currents: The model and its validation," *IEEE Trans. on Power Delivery*, Vol. 14, No. 3, 1008–1017, Jul. 1999.
8. Geri, A., G. M. Veca, E. Garbagnati, and G. Sartorio, "Non-linear behaviour of ground electrodes under lightning surge currents: Computer modeling and comparison with experimental results," *IEEE Trans. on Magnetics*, Vol. 28, No. 2, 1442–1445, Mar. 1992.
9. Zhang, B., J. He, J.-B. Lee, X. Cui, Z. Zhao, J. Zou, and S.-H. Chang, "Numerical analysis of transient performance of grounding systems considering soil ionization by coupling moment method with circuit theory," *IEEE Trans. on Magnetics*, Vol. 41, No. 5, 1440–1443, May 2005.
10. Habjanic, A. and M. Trlep, "The simulation of the soil ionization phenomenon around the grounding system by the finite element method," *IEEE Trans. on Magnetics*, Vol. 42, No. 4, 867–870, Apr. 2006.
11. Mohamad, N. N., A. Haddad, and H. Griffiths, "Characterization of ionization phenomena in soils under fast impulses," *IEEE*

Trans. on Power Delivery, Vol. 21, No. 1, 353–361, Jan. 2006.

12. Zeng, R., X. Gong, J. He, B. Zang, and Y. Gao, "Lightning impulse performance of grounding grids for substations considering soil ionization," *IEEE Trans. on Power Delivery*, Vol. 23, No. 2, 667–675, Apr. 2008.
13. Bellaschi, P. L., "Impulse and 60-cycle characteristics of driven grounds," *Trans. Am. IEE*, Vol. 60, 123–128, 1941.
14. Liew, A. C. and M. Darveniza, "Dynamics model of impulse characteristics of concentrated earth," *Proc. IEE*, Vol. 121, No. 2, 123–135, Feb. 1974.
15. Kenneth, J. N., I. R. Jandrell, and A. J. Phillips, "A simplified model of the lightning performance of a driven rod earth electrode in multi-layer soil that includes the effect of soil ionisation," *Industry Applications Conference. 41st IAS Annual Meeting. Conference Record of the 2006 IEEE*, Vol. 4, 1821–1825, 2006.
16. Liew, A. C., J. Wang, and M. Darveniza, "Extension of dynamic model of impulse behaviour of concentrated earths at high currents," *IEEE Trans. on Power Delivery*, Vol. 20, No. 3, 2160–2165, Jul. 2005.
17. Liu, Y., N. Theethayi, R. Thottappillil, R. M. Gonzales, and M. Zitnik, "An improved model for soil ionization around grounding system and its application to stratified soil," *Journal of Electrostatics*, Vol. 60, No. 2–4, 203–209, Mar. 2004.
18. Sekioka, S., M. I. Lorentzou, M. P. Philippakou, and J. M. Prousalidis, "Current dependent grounding resistance model based on energy balance of soil ionization," *IEEE Trans. on Power Delivery*, Vol. 21, No. 1, 194–201, Jan. 2006.
19. Leadon, R. E., T. M. Flanagen, C. E. Mallon, and R. Denson, "Effect of ambient gas on ARC initiation characteristics in soil," *IEEE Trans. on Nuclear Science*, Vol. 30, No. 6, 4572–4576, Nov. 1983.
20. Ala, G., P. L. Buccheri, P. Romano, and F. Viola, "Finite difference time domain simulation of earth electrodes soil ionization under lightning surge condition," *IET Science, Measurement and Technology*, Vol. 2, No. 3, 134–145, May 2008.
21. Cooray, V., M. Zitnik, M. Manyahi, R. Montano, M. Rahman, and Y. Liu, "Physical model of surge current characteristics of buried vertical rods in the presence of soil ionization," *Journal of Electrostatics*, Vol. 60, No. 2–4, 193–202, Mar. 2004.
22. Mousa, A. M., "The soil ionization gradient associated with discharge of high currents into concentrated electrodes," *IEEE*

Trans. on Power Delivery, Vol. 9, 1669–1677, Jul. 1994.

23. D'Angola, A., M. Capitelli, G. Colonna, and C. Gorse, "Transport properties of high temperature air in local thermodynamic equilibrium," *The European Physical Journal D, Atomic, Molecular, Optical and Plasma Physics,* Vol. 11, No. 2, 279–289, Jul. 2000.
24. Capitelli, M., G. Colonna, and A. D'Angola, "Thermodynamic properties and transport coefficients of high temperature air," *Pulsed Power Plasma Science. PPPS-2001. Digest of Technical Papers,* Vol. 1, No. 17–22, 694–697, Jun. 2001.
25. Prager, J., G. Baldea, U. Riedel, and J. Warnatz, "Equilibrium composition and electrical conductivity of high-temperature air," *21st ICDERS*, 23–27, Poitiers, France, Jul. 2007.
26. Yee, K. S., "Numerical solution of initial boundary value problems involving Maxwell's equations in isotropic media," *IEEE Trans. on Antennas and Propagation*, Vol. 14, 302–307, 1966.
27. Taflove, A. and S. Hagness, *Computational Electro Dynamics: The Finite-difference Time-domain Method*, Artech House, Boston, MA, 2000.
28. Sullivan, D. M., *Electromagnetic Simulation Using the FDTD Method*, IEEE Press Series on RF and Microwave Technology, Jul. 2000.
29. Cassie, A. M., "Arc rupture and circuit severity: A new theorie," CIGRE Report, No. 102, Paris, France, 1939.
30. Noda, T. and S. Yokoyama, "Thin wire representation in finite difference time domain surge simulation," *IEEE Trans. on Power Delivery*, Vol. 17, No. 3, 840–847, Jul. 2002.